J|A|C|S

A R T I C L E S

Thermodynamics, Kinetics, and Dynamics of the Two Alternative Aniomesolytic Fragmentations of C–O Bonds: An Electrochemical and Theoretical Study

Luisa Pisano,[†] Maria Farriol, Xavier Asensio, Iluminada Gallardo, Angels González-Lafont, José M. Lluch,* and Jordi Marquet*

Contribution from the Departament de Química, Universitat Autònoma de Barcelona, 08193 Bellaterra, Barcelona, Spain

Received October 26, 2001

Abstract: Fragmentation reactions of radical anions (mesolytic cleavages) of cyanobenzyl alkyl ethers (intramolecular dissociative electron transfer, heterolytic cleavages) have been studied electrochemically. The intrinsic barriers for the processes have been established from the experimental thermodynamic and kinetic parameters. These values are more than 3 kcal/mol lower as an average than the related homolytic mesolytic fragmentations of radical anions of 4-cyanophenyl ethers. In the particular case of isomers 4-cyanobenzyl phenyl ether and 4-cyanophenyl benzyl ether, the difference in intrinsic barriers amounts to 5.5 kcal/mol, and this produces an energetic crossing where the thermodynamically more favorable process (homolytic) is the kinetically slower one. The fundamental reasons for this behavior have been established by means of theoretical calculations within the density functional theory framework, showing that, in this case, the factors that determine the kinetics are clearly different (mainly present in the transition state) from those that determine the thermodynamics and they are not related to the regioconservation of the spin density ("spin regioconservation principle"). Our theoretical results reproduce quite well the experimental energetic difference of barriers and demonstrate the main structural origin of the difference.

1. Introduction

Unimolecular fragmentation of radical ions to yield radicals and ions (mesolytic cleavages) constitutes an elementary step of many electron-transfer-initiated processes of chemical and biochemical interest.[1] The rates of these reactions are usually significantly faster than those observed for the homolytic cleavage of the same bonds in neutral substrates.[2,3] In aryl and benzyl radical anions, especially those substituted with electron-withdrawing groups, bond fragmentation requires that the SOMO electron density be transferred from the π^* system of the aryl ring to the region between the two atoms of the scissile bond. Some authors have considered mesolytic cleavages as intramolecular electron transfers and have modeled their dynamics in the framework of Marcus theory.[4] The energy barriers associated with mesolytic cleavages have been proposed to be the result of electron redistribution and/or solvent reorganization, allowing them to be used as experimental probes of the kinetics
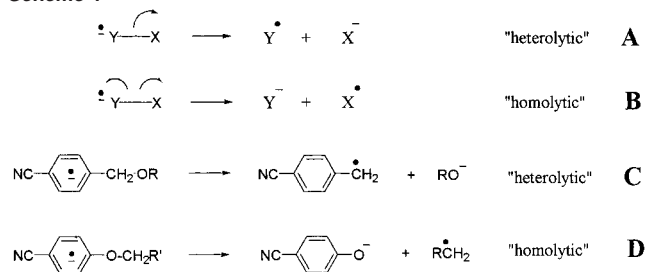
and thermodynamics of these elementary reactions, especialy the identification of the factors contributing to the intrinsic barriers.[5,6]

In the fragmentation of radical ions wherein the unpaired electron resides initially in a π orbital on one side of the scissile bond, electron reapportionment can occur with transfer of charge across the scissile bond (heterolytic mode, Scheme 1A), or the charge may remain localized on the original moiety (homolytic mode, Scheme 1B). Maslak et al. proposed the empirical "spin regioconservation principle" from studies on aryl benzyl ethers[7]

Scheme 1

* Corresponding authors: fax (+34)935811265; e-mail jordi.marquet@uab.es.

† On leave from the Università di Sassari (Italy).

(1) (a) Savéant, J.-M. *Tetrahedron* **1994**, *50*, 10117. (b) Maslak, P. *Top. Curr. Chem.* **1993**, *168*, 1. (c) Savéant, J.-M. *Acc. Chem. Res.* **1993**, *26*, 455. (d) Sancar, A. *Biochemistry* **1994**, *33*, 2.

(2) Chanon, M.; Rajzmann, M.; Chanon, F. *Tetrahedron* **1990**, *46*, 6193.

(3) (a) Maslak, P.; Narvaez, J. N.; Vallombroso, T. M., Jr. *J. Am. Chem. Soc.* **1995**, *117*, 12373. (b) Maslak, P.; Narvaez, J. N. *Angew. Chem., Int. Ed. Engl.* **1990**, *29*, 283.

(4) (a) Marcus, R. A. *J. Phys. Chem.* **1965**, *43*, 679. (b) Kojima, H.; Bard, A. J. *J. Am. Chem. Soc.* **1975**, *97*, 6317. (c) Eberson, L. *Electron-Transfer Reactions in Organic Chemistry*; Springer: Berlin, 1987.

(5) (a) Savéant, J.-M. Dissociative Electron Transfer. In *Advances in Electron-Transfer Chemistry*; Mariano, P. S., Ed.; JAI Press: New York, 1994; Vol. 4, pp 53–116. (b) Savéant, J.-M. *J. Am. Chem. Soc.* **1987**, *109*, 6755. (c) Savéant, J.-M. *J. Phys. Chem.* **1994**, *98*, 3716.

(6) (a) Maslak, P. *Top. Curr. Chem.* **1993**, *168*, 1. (b) Maslak, P.; Vallombroso, T. M., Jr.; Chapman, W. H., Jr.; Narvaez, J. N. *Angew. Chem., Int. Ed. Engl.* **1994**, *33*, 73. (c) Maslak, P.; Narvaez, J. N.; Kula, J.; Malinski, D. S. *J. Org. Chem.* **1990**, *55*, 4550.

(7) (a) Maslak, P.; Guthrie, R. D. *J. Am. Chem. Soc.* **1986**, *108*, 2628. (b) Maslak, P.; Guthrie, R. D. *J. Am. Chem. Soc.* **1986**, *108*, 2637.

and thioethers,[8] arguing that an extra intrinsic barrier exists for the homolytic cleavage, which does not regioconserve spin density. The difference in reactivity between the two modes of fragmentation has been attributed in the literature (on the basis of studies on C–C and C–S bond fragmentations) to the delocalization of charge in the transition state[8,9] and to the influence of solvent reorganization.[10]

Although there are extensive quantitative data on the mechanisms of carbon–halogen bond cleavage by electrochemical means,[11] and significant contributions to the mechanistic knowledge on aniomesolytic C–C[3,6], O–O[9], and C–S[8,12] cleavages, to our knowledge no reports exist in the literature about the fundamental reasons for the very different behavior of the homolytic and heterolytic modes of aniomesolytic fragmentation for highly polarized strong bonds such as the C–O bond in ethers (where first this distinct behavior was experimentally observed). Indeed, even though preparative useful examples of carbon–oxygen bond reductive cleavage in ethers have been reported,[13] very few mechanistic studies exist, either chemical[14] or electrochemical,[15] and the available kinetic data are very scarce. On the basis of a kinetic isotope effects study on naphthyl ethers, the involvement of a π^* transition state in the heterolytic mesolytic cleavage, and of a σ^* transition state in the homolytic mesolytic cleavage, has been proposed.[14b] Very recently some of us have described the thermodynamics and kinetics of the homolytic cleavage of carbon–oxygen bonds in anion radicals obtained by electrochemical reduction of cyanophenyl ethers.[10b] We present here the thermodynamics and kinetics of the heterolytic electroreductive cleavage of related cyanobenzyl ethers and show that, for mesolysis of C–O bonds, the intrinsic barriers of the heterolytic mode are substantially lower (more than 3 kcal/mol) than those of the homolytic mode.

To get some insight on the fundamental reasons for the differences in kinetic behavior between the homolytic and the heterolytic mesolytic fragmentation modes, we have carried out a theoretical study in the gas phase, within the framework of density functional theory (DFT) for the 4-cyanophenyl benzyl
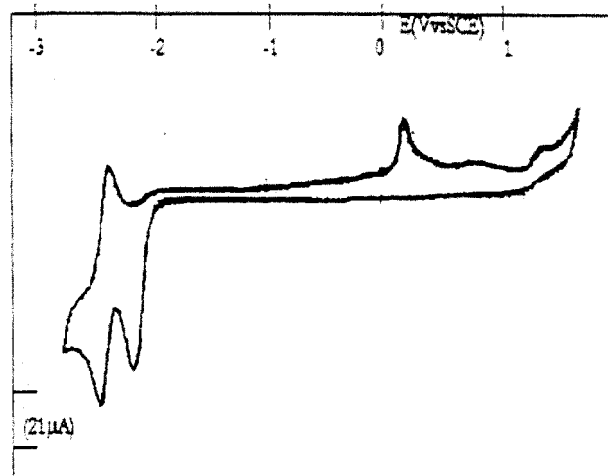

Figure 1. Voltammogram of 4-cyanobenzyl phenyl ether (**1a**) in DMF (10 mM) and 0.1 M TBATFB, at 0.1 V/s. Glassy carbon disk electrode (3 mm diameter). Scan potential range: 0.00/−2.75/+1.50/0.00 V.

ether and 4-cyanobenzyl phenyl ether, isomers that only differ structurally in the orientation of the C–O bond but that show a very significant difference in intrinsic barrier for mesolytic cleavage (Scheme 1C,D). Our theoretical results confirm the main structural origin of the experimental energetic difference of barriers.

It is very surprising that despite the importance of the processes that involve the cleavage of formal three-electron bonds in aromatic derivatives, very few theoretical studies have been performed on them. A series of well-established empirical rules, and the qualitative use of the "reactive mixed-valence approach" are the customary tools in predicting the organic reactivity in this particular field.[2,4c,16,17] Theoretical molecular orbital (MO) ab initio investigation of the reductive C–Cl bond cleavage in nonsubstituted benzyl derivatives led to the conclusion that the corresponding radical anions show a dissociative behavior.[18a] However, recent density functional theory (DFT) calculations reveal the formation of radical anions in these systems.[18b] DFT has been applied also very recently to the study of the photoenzymic repair mechanism that includes a step of cleavage of a radical anion.[19] As far as we know, DFT methodology has not previously been applied to the study of the reductive cleavage of highly polar and strong C–X bonds such as C–O bonds.

2. Experimental Results

2.1. Electrochemical Measurements. Figure 1 shows a typical voltammogram of 4-cyanobenzyl phenyl ether (**1a**), at slow sweep rate (0.1 V s^{−1}), in DMF. A bielectronic irreversible reduction wave ($E_{pc(I)} = -2.20$ V) can be observed. In these conditions, another reduction wave, reversible and monoelec-

(8) Maslak, P.; Theroff, J. *J. Am. Chem. Soc.* **1996**, *118*, 7235.
(9) (a) Donkers, R. L.; Maran, F.; Wayner, D. D. M.; Workentin, M. S. *J. Am. Chem. Soc.* **1999**, *121*, 7239. (b) Sabrina, A.; Martin, M.; Wayner, D. D. M.; Maran, F. *J. Am. Chem. Soc.* **1997**, *119*, 9541. (c) Workentin, M. S.; Maran, F.; Wayner, D. D. M. *J. Am. Chem. Soc.* **1995**, *117*, 2120.
(10) (a) Andrieux, C. P.; Savéant, J.-M.; Tallec, A.; Tardivel, R.; Tardy, C. *J. Am. Chem. Soc.* **1996**, *118*, 9788. (b) Andrieux, C. P.; Farriol, M.; Gallardo, I.; Marquet, J. *J. Chem. Soc., Perkin Trans. 2*, in press.
(11) (a) Savéant, J.-M. Electron Transfer, Bond Breaking and Bond Formation. In *Advances in Physical Organic Chemistry*; Tidwell, T. T., Ed.; Academic Press: New York, 2000; Vol. 35, p 117. (b) Andrieux, C. P. Organic Electrochemical Mechanisms. In *Encyclopedia of Analytical Chemistry*; Wiley: Chichester, U.K., 2000; p 9983.
(12) (a) Screttas, C. G.; Screttas, M. M. *J. Org. Chem.* **1978**, *43*, 1064. (b) Cohen, T.; Buphaty, M. *Acc. Chem. Res.* **1989**, *22*, 152. (c) Severin, M. G.; Arevalo, M. C.; Farnia, G.; Vianello, E. *J. Phys. Chem.* **1987**, *91*, 466.
(13) (a) Maercker, A. *Angew. Chem., Int. Ed. Engl.* **1987**, *26*, 972 and references therein. (b) Azzena, U.; Denurra, T.; Melloni, G.; Piroddi, A. M. *J. Org. Chem.* **1990**, *55*, 5386. (c) Azzena, U.; Melloni, G.; Pisano, L.; Sechi, B. *Tetrahedron Lett.* **1994**, *35*, 6759. (d) Marquet, J.; Cayón, E.; Martín, X.; Casado, F.; Gallardo, I.; Moreno, M.; Lluch, J. M. *J. Org. Chem.* **1995**, *60*, 3814.
(14) (a) Lazana, M. C. R. L. R.; Franco, M. L. T. M. B.; Herold, B. J. *J. Am. Chem. Soc.* **1989**, *111*, 8640. (b) Guthrie, R. D.; Shi, B. *J. Am. Chem. Soc.* **1990**, *112*, 3136. (c) Cayón, E.; Marquet, J.; Lluch, J. M.; Martin, X. *J. Am. Chem. Soc.* **1991**, *113*, 8970. (d) Azzena, U.; Denurra, T.; Melloni, G.; Fenude, E.; Rassu, G. *J. Org. Chem.* **1992**, *57*, 1444. (e) Gonzalez-Blanco, R.; Bourdelande, J. L.; Marquet, J. *J. Org. Chem.* **1997**, *62*, 6910. (f) Saá, J. M.; Ballester, P.; Deyá, P. M.; Capó, M.; Garcías, X. *J. Org. Chem.* **1996**, *61*, 1035. (g) Casado, F.; Pisano, L.; Farriol, F.; Gallardo, G.; Marquet, J.; Melloni, G. *J. Org. Chem.* **2000**, *65*, 322.
(15) (a) Thornton, T. A.; Ross, G. A.; Patil, D.; Mukaida, K.; Warwick, J. O.; Woolsley. N. F.; Bartak, D. E. *J. Am. Chem. Soc.* **1989**, *111*, 8640. (b) Andersen, M. L.; Long, W.; Wayner, D. D. M. *J. Am. Chem. Soc.* **1997**, *119*, 6590.

(16) (a) Symons, M. C. R. *Pure Appl. Chem.* **1981**, *53*, 223. (b) Bunnett, J. F.; Creary, X. *J. Org. Chem.* **1975**, *40*, 3740. (c) Villar, H.; Castro, E. A.; Rossi, R. A. *Can. J. Chem.* **1982**, *60*, 2525.
(17) (a) Moreno, M.; Gallardo, I.; Bertrán, J. *J. Chem. Soc., Perkin Trans. 2* **1989**, 2017. (b) Martin, X.; Marquet, J., Lluch, J. M. *J. Chem. Soc., Perkin Trans. 2* **1993**, 87. (c) Pierini, A. B.; Duca, J. S., Jr. *J. Chem. Soc., Perkin Trans. 2* **1995**, 1821. (d) Voityuk, A. A.; Michel-Beyerle, M.-E.; Rösch, N. *J. Am. Chem. Soc.* **1996**, *118*, 9750. (e) Pierini, A. B.; Duca, J. S., Jr.; Vera, D. M. A. *J. Chem. Soc., Perkin Trans. 2* **1999**, 1003.
(18) (a) Benassi, R.; Bertarini, C.; Taddei, F. *J. Chem. Soc., Perkin Trans. 2* **1997**, 2263. (b) Dem'yanov, P. I.; Myshakin, E. M.; Boche, G.; Petrosyan, V. S.; Alekseiko, L. N. *J. Phys. Chem. A* **1999**, *103*, 11469.
(19) Durbeej, B.; Eriksson, L. A. *J. Am. Chem. Soc.* **2000**, *122*, 10126.
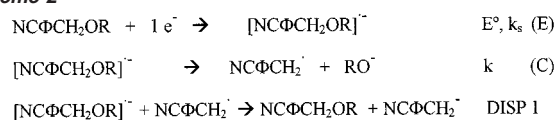
Scheme 2

$$NC\Phi CH_2OR \ + \ 1\,e^- \ \rightarrow \ [NC\Phi CH_2OR]^{\bullet -} \qquad E^\circ, k_s \ \ (E)$$

$$[NC\Phi CH_2OR]^{\bullet -} \ \rightarrow \ NC\Phi CH_2^{\bullet} \ + \ RO^- \qquad k \ \ (C)$$

$$[NC\Phi CH_2OR]^{\bullet -} + NC\Phi CH_2^{\bullet} \rightarrow NC\Phi CH_2OR \ + NC\Phi CH_2^{\bullet} \quad DISP\ 1$$

Table 1. Reactivity Data for the C−O Bond Aniomesolytic Heterolytic Cleavage of Ethers

compound	D (eV)	$-E^\circ_{RX/^{\bullet -}RX}{}^a$	$E^\circ_{X^\bullet/X}{}^a$	ΔG° (eV)	$\log k^b$	$\Delta G_0^{\#}$ (eV)
NCPhCH₂OPh, **1a**	2.23	2.15	0.24^c	−0.363	5.0 ± 0.5	0.655
NCPhCH₂OCH₃, **1b**	2.996^d	2.15	0.54^e	0.013	1.0 ± 0.2	0.673

^{a} Potentials are in volts vs SCE. ^{b} Values from digital simulations of the cyclic voltammetry curves by DigiSim. ^{c} Value taken from ref 24a. ^{d} Calculated from $D_{NCPhCH_2OCH_3} = D_{NCPhCH_2OPh} - D_{PhOH} + D_{CH_3OH}$. ^{e} Value taken from ref 24b.

tronic, placed at potentials slightly more negative than the precedent one ($E^\circ_{(II)} = -2.37$ V) appears. This wave shows the same features than the reduction wave of toluonitrile in dimethylformamide (DMF) (the same potential, reversible at any sweep rate, and monoelectronic), and therefore it is assigned to the reduction of this compound, formed by reductive cleavage of the alkyl ether bond (see the preparative electrolysis described below). At positive potentials, and only at low sweep rates, it is possible to observe after the reduction of **1a**, a small oxidation wave at 0.25 V. This anodic wave would correspond to the oxidation of the phenoxide anion (0.24 V in acetonitrile).[20] Voltammograms of 4-cyanobenzyl methyl ether (**1b**) are very similar ($E_{pc(I)} = -2.24$ V, $E^\circ_{(II)} = -2.37$ V). Analysis of the first reduction peak intensity indicates the existence of a two-electron process at low sweep rates and one-electron process at high sweep rates (>2 × 10⁴ V s⁻¹ for **1a** and >2 V s⁻¹ for **1b**).

The shape of voltammograms (peak width) suggests, in both cases, a mixed kinetic control by electron transfer and a coupled chemical reaction.[21] The peak potential is not concentration-dependent (in the range 1−10 mM) and the variation of the peak potential with the scan rate is 30 mV by unit log scan rate for low scan rates.[21] Therefore, we can conclude that the initially produced radical anion reacts following a slow first-order reaction pathway leading to a second electron transfer following a DISP 1 mechanism (Scheme 2).[22] At a low sweep rate, reaction 1 of Scheme 2 is followed by reactions 2 and 3 (two electrons altogether). At a fast sweep rate, only the reversible formation of cyanobenzyl ether radical anion would be observed (reaction 1 of Scheme 2; one-electron reversible process). This conclusion was confirmed by digital simulations of the cyclic voltammetry curves, with DigiSim software, that allowed a reliable determination of the standard potentials for the formation of the radical anions of **1a** and **1b** and their cleavage rate constants (Table 1).

Electrolysis of 4-cyanobenzyl phenyl ether (**1a**) and 4-cyanobenzyl methyl ether (**1b**) were carried out until $2F$, at a potential slightly more negative than the peak potential for each one. In the case of **1a**, 25% of the starting material was recovered, and 24% toluonitrile and 40% phenol were obtained. In the case of

(20) (a) Hapiot, P.; Pinson, J.; Yousfi, N. *New J. Chem.* **1992**, *16*, 877. (b) Eberson, L. *Acta Chem. Scand.* **1984**, *B38*, 439.
(21) (a) Nadjo, L. Savéant, J.-M. *J. Electroanal. Chem.* **1973**, 48, 113. (b) Andrieux, C. P.; Savéant, J.-M. Electrochemical Reactions. In *Investigation of Rates and Mechanism of Reactions*; Techniques of Chemistry; Bernasconi, C. F., Ed.; Wiley: New York, 1986; Vol 6, Chapter 2.1, p 305.
(22) Amatore, C.; Savéant, J.-M. *J. Electroanal. Chem.* **1980**, *107*, 353.

1b, 40% of the starting material was recovered, and 60% toluonitrile was obtained (methanol was not quantified). Analysis of the electrolyzed solutions by electrochemical and chromatographic techniques indicated that no cyanobenzyl alcohol was formed (the only ether bond cleavage observed corresponds to the cyanobenzyl ether bond). With different solvents (DMF, ACN, or THF) and different salts (TBABF₄, LiClO₄) as supporting electrolytes, no significant changes on the cleavage rates, standard potentials, and nature and yields of products were observed. Therefore, in these cases, the effect of solvation and ion pairing seems negligible.

Electrochemical reduction results for the cyanobenzyl phenyl, **1a**, and cyanobenzyl methyl, **1b**, ethers studied are indicative of a mechanism such as the one described in Scheme 2. The radical anion resulting from single electron transfer to an aromatic ether is a frangible species that decomposes readily. In the radical anion, the unpaired electron must be located initially in the cyanophenyl moiety of the molecule since its standard potential is very close to that of benzonitrile. The cleavage of the bond leads to NCPhCH₂• and RO⁻ and thus involves a "mesolytic heterolytic" dissociation (intramolecular dissociative electron transfer) of the benzylic C−O bond in the radical anion •⁻NCPhCH₂OR. The final reduction of NCPhCH₂• will probably take place in solution by another radical anion due to the relatively low value of the cleavage rate constant (DISP 1 mechanism).[21,22]

2.2. Thermodynamics and Kinetics of Mesolytic Heterolytic Bond Cleavage in Cyanobenzyl Alkyl Ethers. We have just demonstrated that the bond cleavage between the oxygen and the benzylic carbon step in the reduction of 4-cyanobenzyl phenyl ether (**1a**) and 4-cyanobenzyl methyl ether (**1b**) leads to heterolytic dissociation:

$$^{\bullet -}(NCPhCH_2OR) \rightarrow NCPhCH_2^{\bullet} + RO^- \qquad (1)$$

To obtain the thermodynamic and kinetic details of this process we follow the model for cleavage of radical anions described by Savéant[5] in the framework of the Marcus theory. Thus, the standard free energy, ΔG°, for the overall reaction (eq 1) is

$$\Delta G^\circ = D_{(RX)} + E^\circ_{(RX/RX^{\bullet -})} - E^\circ_{(X^\bullet/X^-)} - T\Delta S \qquad (2)$$

with R = NCPhCH₂ and X = R′O in our case.

The activation free energy, $\Delta G^{\#}$ (in electronvolts), is calculated by the Eyring equation (eq 3), taking the preexponential factor equal to 5 × 10¹² s⁻¹:[1a]

$$\log k = \log A - (F/2.303RT)\Delta G^{\#} \qquad (3)$$

The activation free energy, $\Delta G^{\#}$, is related quadratically to the standard free energy of the reaction, ΔG°:

$$\Delta G^{\#} = \Delta G_0^{\#} (1 + \Delta G^\circ/4\Delta G_0^{\#})^2 \qquad (4)$$

The term $\Delta G_0^{\#}$ is the intrinsic barrier free energy.

The cleavage rate constant of the radical anions and the standard potential for the formation of the radical anions of **1a** and **1b** were derived from our cyclic voltammetric data by digital simulation of the curves with DigiSim. The standard redox potentials of the leaving anions were taken from the literature[20] (see Table 1). The value corresponding to the

Table 2. Comparison of the Thermodynamic and Kinetic Parameters for the Two Alternative C−O Bond Aniomesolytic Fragmentations of Alkyl Ethers[a]

type of cleavage	compound	$\Delta G°$	log k	$\Delta G^{\#}$	$\Delta G_0^{\#}$
"heterolytic"	NCPhCH$_2$OPh, **1a**	−10.45	5.0 ± 0.5	10.3	15.1
	NCPhCH$_2$OCH$_3$, **1b**	0.30	1.0 ± 0.2	15.7	15.5
"homolytic"[b]	NCPhOCH$_2$Ph, **2**	−16.67	2.9 ± 0.2	13.1	20.6
	NCPhOCH$_2$CHCH$_2$, **3**	−13.67	3.1 ± 0.2	12.9	19.1
	NCPhOCH$_3$, **4**	−2.83	1.0 ± 0.2	15.7	17.2
	NCPhO(CH$_2$)$_2$CHCH$_2$, **5**	−2.37	0.7 ± 0.2	16.1	17.2

[a] Energies are given in kilocalories per mole; k is given in reciprocal seconds. [b] Values from ref 10b.

variation of entropy in eq 2 has been taken as 1 meV/K.[23] The values used, and the results obtained, for the thermodynamic and kinetic parameters for compounds **1a** and **1b** are shown in Table 1.

2.3. Discussion of the Experimental Results: Mesolytic Heterolytic vs Mesolytic Homolytic Fragmentations. As indicated in the Introduction, some of us have very recently[10b] described the thermodynamics and kinetics of the mesolytic homolytic cleavage of a series of cyanophenyl alkyl ethers, and it was our intention to compare these reported thermodynamic and kinetic parameters with the ones described here for the mesolytic heterolytic cleavage of cyanobenzyl methyl and phenyl ethers. In Table 2, the thermodynamic and kinetic parameters for the reductive cleavage of compounds **1a** and **1b** are compared with the corresponding values for some selected cyanophenyl alkyl ethers (compounds **2−5**).[10b] From the table, it comes that despite the variability of thermodynamic driving forces for the studied reactions (spanning from $\Delta G° = +0.30$ to −16.67 kcal/mol), a relatively narrow range of intrinsic barrier values is obtained for each series of compounds. Compounds that show heterolytic mesolytic cleavages (**1a** and **1b**) have a lower intrinsic barrier (15.3 kcal/mol as an average) than the ones that show homolytic mesolytic fragmentation (**2**, **3**, **4**, and **5**; 18.53 kcal/mol as an average). This differential behavior (more than 3 kcal/mol) is independent of the thermodynamics and seems to be due to fundamental differences between both types of cleavages. A very related behavior has been described for C−S fragmentations.[8]

It is especially interesting to compare the behavior of compounds 4-cyanobenzyl phenyl ether (**1a**) and 4-cyanophenyl benzyl ether (**2**), which are isomers. The difference in intrinsic barrier (5.5 kcal/mol in this case) provokes a crossing in the reaction energetics, such that the thermodynamically more spontaneous process (**2**, homolytic), by a difference of 6.2 kcal/mol, is the slower one by more than 2 orders of magnitude.

3. Theoretical Calculations

As has been shown above, the radical anion of the 4-cyanobenzyl phenyl ether (**1a**) undergoes a faster C−O alkyl ether bond cleavage than the radical anion of the 4-cyanophenyl benzyl ether (**2**) in solution, despite a clear thermodynamic advantage for the latter reaction. To understand this different kinetic behavior and to assess the weight on that of the factors just related to the radical anions themselves (that is, depending on the solute but excluding the contribution of the solvent reorganization), we have theoretically studied both C−O fission

processes in gas phase. In this section we will first provide the calculational details and then the theoretical results.

3.1. Calculational Details. The quantum mechanical calculations have been carried out within the framework of density functional theory (DFT),[26] which is reaching a widespread use in the calculation of quite sizable organic and inorganic molecules. The spin-unrestricted formalism has been used in solving the Kohn−Sham DFT equations.[27] The particular functional used has been the Becke's three-parameter hybrid method with Lee, Yang, and Parr's correlation functional (B3LYP),[28] nowadays one of the most-used functionals. The basis set chosen for the calculations had to be flexible enough to describe anionic species and, therefore, the split valence 6-31+G basis set,[29] which includes a diffuse sp shell on the heavy atoms, has been used. The diffuse functions provide more ample space allowance for the additional electron in the radical anions. It has been shown[30] that the B3LYP method with a moderately large basis set yields electronic spin density ratios in good agreement with experiment.

Full geometry optimization and direct location of stationary points (minima and transition-state structures) have been carried out by means of the Schlegel gradient optimization algorithm by using redundant internal coordinates.[31] Diagonalization of the potential energy analytical second-derivative matrix (Hessian) has been done to disclose the nature of the stationary point of the potential energy surface: no negative eigenvalues indicate a potential energy minimum, whereas one negative eigenvalue identifies a transition-state structure. In this second case, the eigenvector (transition vector) associated with the negative eigenvalue shows the direction along which the potential energy lowers. When it has been required, the minimum energy path (MEP) has been calculated by following the Gonzalez−Schlegel mass-weighted internal coordinates reaction-path algorithm.[32] The MEP goes downhill from the transition-state structure to the two minima at both sides of it. The MEP has been built up with a step size of 0.02 bohr.

Thermodynamic magnitudes have been computed by using the statistical thermodynamic formulation[33] of partition functions within the ideal gas, rigid rotor, and harmonic oscillator models. A pressure of 1 atm and a temperature of 298.15 K have been assumed in the calculations. The analytical second derivatives of the potential energy with respect to the Cartesian coordinates have been used for the determination of vibrational frequencies. The imaginary frequency is neglected in the thermodynamic evaluation for transition-state structures.

The Gaussian 94 and 98 packages[34,35] have been used to carry out all these electronic calculations.

(23) Andrieux, C. P.; Savéant, J.-M.; Tardy, C. *J. Am. Chem. Soc.* **1998**, *120*, 4167.

(24) Maran, F.; Celadon, D.; Severin, M. G.; Vianello, E. *J. Am. Chem. Soc.* **1991**, *113*, 9320.

(25) Bordwell, F. G. *Acc. Chem. Res.* **1988**, *21*, 456.

(26) Kohn, W.; Becke, A. D.; Parr, R. G. *J. Phys. Chem.* **1996**, *100*, 12974.

(27) (a) Hohenberg, P.; Kohn, W. *Phys. Rev. B* **1964**, *136*, 864. (b) Kohn, W.; Sham, L. J. *Phys. Rev. A* **1965**, *140*, 1133.

(28) (a) Becke, A. D. *J. Chem. Phys.* **1993**, *98*, 5648. (b) Becke, A. D. *J. Chem. Phys.* **1996**, *104*, 1040. (c) Becke, A. D. In *Modern Electronic Structure Theory*; Yarkony, D. R., Ed.; World Scientific: Singapore, 1995.

(29) Clark, T.; Chandrasekhar, J.; Spitznagel, G. W.; Shleyer, P. v. R. *J. Comput. Chem.* **1983**, *4*, 294.

(30) Qin, Y.; Wheeler, R. A. *J. Chem. Phys.* **1995**, *102*, 1689.

(31) Peng, C.; Ayala, P. Y.; Schlegel, H. B.; Frisch, M. J. *J. Comput. Chem.* **1996**, *17*, 49.

(32) Gonzalez, C.; Schlegel, H. B. *J. Phys. Chem.* **1990**, *94*, 5523.

(33) McQuarrie, D. A. *Statistical Thermodynamics*; University Science Books: Mill Valley, CA, 1973.
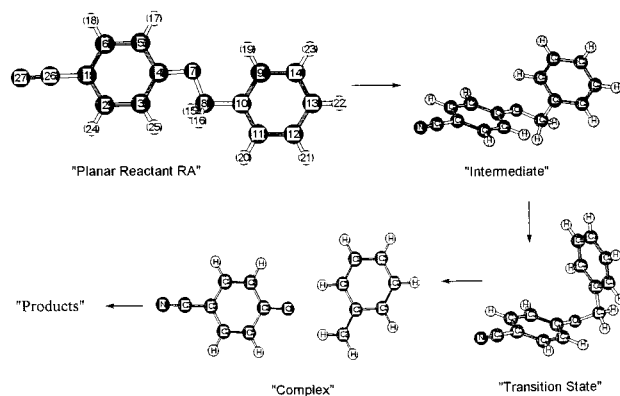
Figure 2. Stationary points in the C−O alkyl ether bond fragmentation of the radical anion of the 4-cyanophenyl benzyl ether (**2**) potential energy surface.

Table 3. Main Geometrical Parameters of the Five Stationary Points Located for the C−O Alkyl Ether Bond Fragmentation of the Radical Anion of 4-Cyanophenyl Benzyl Ether (**2**), along with the Corresponding Potential Energies and Gibbs Free Energies[a]

	$C_8O_7{}^b$	$C_5C_4O_7C_8{}^c$	$C_4O_7C_8C_{10}{}^c$	$O_7C_8C_{10}C_9{}^c$	ΔV^d	$\Delta G°$
reactant	1.441	180.0	180.0	0.0	0.0	0.0
intermediate	1.446	177.3	−78.5	12.9	1.50	1.03
TS	1.481	129.5	−64.6	40.5	2.41	1.21
complex	3.240	1.1	180.7	0.0	−29.1	−33.4
products	∞				−21.7	−34.3

[a] The bond distances, dihedral angles, and energies are given in angstroms, degrees, and kilocalories per mole, respectively. The numbers labeling the nuclei correspond to the ones in Figure 2. [b] Bond distances. [c] Dihedral angles. [d] Potential energy.

3.2. Theoretical Results. To begin with, we will first focus on the C−O alkyl ether bond fragmentation of the radical anion of the 4-cyanophenyl benzyl ether (**2**). We have located five stationary points on the corresponding potential energy surface (Figure 2). With regard to the C−O cleavage, their more relevant geometrical parameters are the scissile C−O bond distance and the three dihedral angles that reflects the relative twisting of the two aromatic rings. They are presented in columns 2−5 of Table 3 (the numbers labeling the nuclei are indicated in the first structure of Figure 2). The last two columns in Table 3 give the potential energy and the Gibbs free energy, respectively, associated with each stationary point, the reactant structure being always taken as the origin of energies.

When one electron is added to neutral 4-cyanophenyl benzyl ether (**2**) to form the corresponding radical anion (the reactant of the C−O fragmentation), the two aromatic rings keep on the
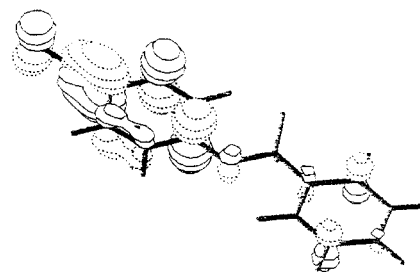
(34) Frisch, M. J.; Trucks, G. W.; Schlegel, H. B.; Gill, P. M. W.; Johnson, B. G.; Robb, M. A.; Cheeseman, J. R.; Keith, T. A.; Petersson, G. A.; Montgomery, J. A.; Raghavachari, K.; Al-Laham, M. A.; Zakrzewski, V. G.; Ortiz, J. V.; Foresman, J. B.; Cioslowski, J.; Stefanov, B. B.; Nanayakkara, A.; Challacombe, M.; Peng, C. Y.; Ayala, P. Y.; Chen, W.; Wong, M. W.; Andres, J. L.; Replogle, E. S.; Gomperts, R.; Martin, R. L.; Fox, D. J.; Binkley, J. S.; Defrees, D. J.; Baker, J.; Stewart, J. P.; Head-Gordon, M.; Gonzalez, C.; Pople, J. A. *Gaussian 94*; Gaussian: Pittsburgh, PA, 1995.
(35) Frisch, M. J.; Trucks, G. W.; Schlegel, H. B.; Scuseria, G. E.; Robb, M. A.; Cheeseman, J. R.; Zakrzewski, V. G.; Montgomery, J. A.; Stratmann, R. E.; Burant, J. C.; Dapprich, S.; Millam, J. M.; Daniels, A. D.; Kudin, K. N.; Strain, M. C.; Farkas, O.; Tomasi, J.; Barone, V.; Cossi, M.; Cammi, R.; Mennucci, B.; Pomelli, C.; Adamo, C.; Clifford, S.; Ochterski, J.; Petersson, G. A.; Ayala, P. Y.; Cui, Q.; Morokuma, K.; Malick, D. K.; Rabuck, A. D.; Raghavachari, K.; Foresman, J. B.; Cioslowski, J.; Ortiz, J. V.; Stefanov, B. B.; Liu, G.; Liashenko, A.; Piskorz, P.; Kamaromi, I.; Gomperts, R.; Martin, R. L.; Fox, D. J.; Keith, T.; Al-Laham, M. A.; Peng, C. Y.; Nanayakkara, A.; Gonzalez, C.; Challacombe, M.; Gill, P. M. W.; Johnson, B. G.; Chen, W.; Wong, M. W.; Andres, J. L.; Head-Gordon, M.; Replogle, E. S.; Pople, J. A. *Gaussian 98*; Gaussian: Pittsburgh, PA, 1998.

Figure 3. Occupied π^* molecular spin orbital of the radical anion of the 4-cyanophenyl benzyl ether (**2**).

molecular plane as indicated by the dihedral angles in Table 3, and a π^* molecular spin orbital (HSOMO) becomes occupied (Figure 3).

From the geometrical point of view, the extra electron shortens the scissile C−O bond from 1.460 Å at the neutral molecule to 1.441 Å at the radical anion. Then, rather surprisingly, we observe that the extra electron compresses the scissile bond, which initially evolves in the opposite sense to what could be expected at first glance.

Our theoretical results indicate that the electronic ground state for the radical anion of the 4-cyanophenyl benzyl ether (**2**) is a π^* state with the extra electron concentrated on the cyanophenyl part of the molecule and on the oxygen atom. This state is not appropriate to produce the C−O alkyl ether bond fragmentation. Then an intramolecular electron transfer from the π^* ground state to a suitable excited state has to occur prior to the experimentally observed C−O bond cleavage. This will be a σ^* electronic excited state (at the reactant) that involves the occupation of a σ^* antibonding C−O alkyl ether molecular spin orbital. Assuming a classical frame, the radiationless electron transfer must take place at the intersection region of the diabatic potential energy surfaces corresponding to the π^* and σ^* diabatic states. Random thermal fluctuations in the nuclear configurations of the radical anion in the π^* state, involving especially the lengthening of the C−O alkyl ether bond, occur until that intersection region is reached; then the energies of both diabatic states become equal and the electron jump happens. After the intramolecular electron transfer the C−O bond, already in the σ^* state, dissociates directly. The appearance of the proper fluctuations costs free energy. It is this free energy that determines the rate of the fragmentation process. Likewise, the classical energy barrier arises from the potential energy required to deform the radical anion in the π^* state up to the minimum energy structure of the intersection region (the transition-state structure).

To locate the transition-state structure we have stretched the C−O alkyl ether bond of the radical anion of the 4-cyanophenyl benzyl ether (**2**). For each value of the C−O distance, the rest of the geometrical parameters of the molecule have been optimized in order to minimize the energy. The energy grows monotonically with the C−O distance, in such a way that no maximum energy point (the transition-state structure) appears, at least before a C−O distance of 1.85 Å. However, a careful analysis of the calculations reveals that the set of geometrical structures associated with that energy profile keeps the planarity of the molecule. As a consequence, two kind of geometrical distortions are required to achieve the fragmentation: the C−O alkyl ether stretching and the twisting of the two rings away from planarity. Taking all this into account, we have followed

the evolution (to reactant or to products) of some of the planar structures when they are allowed to relax after some slight deviation from planarity has been introduced. Direct location of the transition state from the planar structure with a scissile C—O bond distance of 1.55 Å led to the structure whose main geometrical parameters are given in the third row of Table 3. At this transition-state structure the C—O bond becomes 0.04 Å longer than in the reactant. On the other hand, the molecule is now clearly far from planarity (see Figure 2). In particular, the $C_5C_4O_7C_8$ dihedral angle (129.5°) carries the scissile C_8–O_7 bond to a position orthogonal to, rather than coplanar with, the cyanophenyl ring, in this way trying to maximize the overlap between the π system of the cyanophenyl ring and the σ system of the C—O alkyl ether bond. As a result of all these distortions, the classical energy barrier turns out to be 2.41 kcal/mol.

The transition vector (that is, the eigenvector of the Hessian associated with the unique negative eigenvalue that, as a consequence, indicates the direction in which the potential energy goes downhill) turns out to be a mixing of the variation of the C_8–O_7 bond distance and the twisting of the dihedral angles, showing the kind of nuclear motions that make possible the C—O fragmentation.

From the transition-state structure the MEP toward the reactant leads to a minimum energy structure (Figure 2) that is an intermediate of the C—O scission and whose main geometrical parameters are given in the second row in Table 3. At this intermediate the cleavage of the C—O alkyl ether bond has not begun yet; its main geometrical difference with regard to the reactant consists of the change of the $C_4O_7C_8C_{10}$ dihedral angle, which raises the benzyl ring well above the plane of the rest of the molecule. As a consequence, the intermediate appears only 1.5 kcal/mol above the reactant. Conversely, the MEP toward the products does not converge, probably due to the jump of the molecule between the two electronic states, which are very close near the transition-state structure. Anyway, if the molecule is allowed to relax after the C_8–O_7 bond has been lengthened 0.1 Å, the C—O scission takes place, reaching a complex (fourth row in Table 3, Figure 2), 29.1 kcal/mol below the reactants, composed of two fragments: the cyanophenolate anion and the benzyl radical. In this complex the C_8–O_7 alkyl ether bond is already broken (3.240 Å). On going to the final separated products, the potential energy rises 7.4 kcal/mol.

Let us describe in short the movements during the fragmentation of the radical anion of the 4-cyanophenyl benzyl ether. First, from the planar reactant to the intermediate, the scissile C_8–O_7 bond does not lengthen and it remains coplanar with the cyanophenyl ring, whereas the benzyl ring rises up to an almost perpendicular conformation. At the transition-state structure the C_8–O_7 bond becomes slightly stretched and it goes far from the plane of the cyanophenyl ring in order to permit the HSOMO to have a significant C—O σ^* contribution, which will lead to the C—O alkyl ether scission. In Figure 4, the evolution of the net atomic charges along the reaction coordinate is described. These charges derive from the natural atomic orbitals and are obtained from a natural population analysis (NPA) according to the procedure developed by Weinhold and co-workers.[36] In Figure 4, the evolution of the NPA spin distribution (that is,
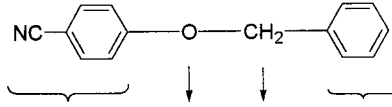

CHARGE	**A**	**B**	**C**	**D**
Neutral Reactant	0.197	-0.530	0.342	-0.020
Planar Radical Anion	-0.508	-0.554	0.295	-0.235
Intermediate	-0.501	-0.558	0.316	-0.257
TS	-0.496	-0.577	0.302	-0.228
SPIN				
Planar Radical Anion	0.766	0.013	0.000	0.224
Intermediate	0.756	0.017	0.003	0.214
TS	0.761	0.012	0.031	0.201

Figure 4. NPA net atomic charges (in au) for neutral 4-cyanophenyl benzyl ether (**2**), the corresponding radical anion, the intermediate, and the transition state of the C—O fragmentation and NPA spin distribution (in au) for the radical anion of the 4-cyanophenyl benzyl ether (**2**), the intermediate, and the transition state of the C—O fragmentation.
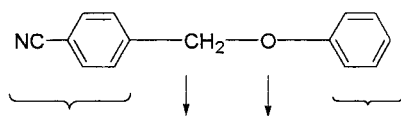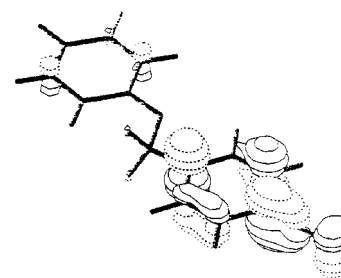

Figure 5. Occupied π^* molecular spin orbital of the radical anion of the 4-cyanobenzyl phenyl ether (**1a**).

the difference between the α and β NPA net atomic charges) is also given. It can be seen that the additional negative charge in the radical anion lies for the most part on the cyanophenyl atoms and the oxygen atoms and that, on going from the planar radical anion to the transition state, a transfer of charge from the phenyl rings to the scissile bond atoms (C—O) is observed. This is even clearer considering the spin distribution change. In this case, the spin density at the benzyl carbon increases significantly, and this agrees with the proposed population of the σ^* spin molecular orbital at the transition state. It is well-known that in a C—O σ bond, the C atom provides the most important contribution to the antibonding σ^* molecular orbital. Once the cleavage has occurred, in the hydrogen-bonded complex the benzyl radical is practically neutral (the total NPA net charge is 0.03 au), but it contains already the whole unpaired electron (the total NPA spin distribution is 1.00 au).

Let us turn our attention to the C—O alkyl ether bond fragmentation of the radical anion of the 4-cyanobenzyl phenyl ether (**1a**). The occupied π^* molecular spin orbital in the radical anion, which is also planar, is depicted in Figure 5. By comparison of Figures 3 and 5, it can be noted that the position of the cyano substituent entirely determines in which ring the HSOMO concentrates.

From the geometrical point of view, the extra electron lengthens the scissile C—O bond from 1.451 Å at the neutral

(36) (a) Reed, A. E.; Weinstock, R. B.; Weinhold, F. *J. Chem. Phys.* **1985**, *83*, 735. (b) Reed, A. E.; Curtiss, L. A.; Weinhold, F. *Chem. Rev.* **1988**, *88* (8), 899.

Figure 6. NPA net atomic charges (in au) for neutral 4-cyanobenzyl phenyl ether (**1a**) and the corresponding radical anion and NPA spin distribution (in au) for the radical anion of the 4-cyanobenzyl phenyl ether (**1a**).

molecule to 1.469 Å at the radical anion. The analysis of the eigenvalues of the Hessian of the radical anion of the 4-cyanobenzyl phenyl ether provides a rather surprising conclusion: this planar structure is not a minimum energy structure but a transition-state structure. The transition vector is a mixture of the twisting of the dihedral angles that breaks the planarity of the molecule, but it does not contain any component corresponding to the variation of the scissile C–O bond distance. In other words, this radical anion is a minimum along the direction corresponding to the C–O bond internal coordinate, but a maximum along the direction that twists the two rings away from planarity. When the geometry is displaced some few degrees along this last direction and then it is allowed to relax, the C–O bond fragments and a complex 13.1 kcal/mol below the transition-state structure is reached. This complex consists of two fragments, the cyanobenzyl radical (the total NPA net charge is still −0.22 au, with a total NPA spin distribution of 0.80 au) and the phenolate anion, with two hydrogen bonds between the oxygen atom and the hydrogen atoms 15 and 16 (the two hydrogen bond lengths are 2.59 Å). The C–O alkyl ether bond length is already 2.65 Å. Separation of the two fragments to reach the products costs 12.5 kcal/mol in terms of potential energy or 3.9 kcal/mol in terms of Gibbs free energy (the difference of magnitude is due to the entropic term, which favors the formation of fragments).

In Figure 6, the net NPA atomic charges for the neutral 4-cyanobenzyl phenyl ether (**1a**) and its radical anion and the NPA spin distribution for the radical anion are shown. In agreement with the finding that the planar radical anion is already a transition state that leads to cleavage of the scissile bond upon a slight twisting of the structure, the benzylic carbon shows a significant spin density (0.043 au; compare with the transition state of compound **2**, Figure 4).

Let us rationalize now the different behavior of the two radical anions. The first striking difference is the fact that the uptake of one electron (planar radical anion) causes a shortening of the C–O scissile bond in the case of cyanophenyl benzyl ether (**2**) and the oposite effect in cyanobenzyl phenyl ether (**1a**). Some hints come from the data of spin distribution gathered in Figures 4 and 6. Thus, in both cases, the planar radical anion shows a significant spin density in the atom directly linked to the cyanophenyl ring (where the main part of the extra electronic density is located). On the other hand, it is well-known that in a C–O bond, the main contribution to a bonding molecular orbital comes from the oxygen atom, whereas the C atom

provides the most important contribution to an antibonding molecular orbital. Then, what is probably happening in the case of **1a** is that when the electron is captured, the scissile C–O bond in the planar radical anion is weakened by increasing the C–O antibonding contribution in the occupied molecular orbitals (spin density in the C atom). As explained above, the molecule dissociates directly when the $\sigma*$ spin molecular orbital of the C–O alkyl ether bond becomes populated. The planar radical anion is just placed at the intersection region, thus, a slight deviation of planarity already introduces components of the antibonding C–O interaction in the $\sigma*$ spin molecular orbital, and the molecule fragments directly. Therefore, the radical anion of **1a** shows purely dissociative behavior, with no Gibbs free energy barrier.

In the case of the cyanophenyl benzyl ether (**2**), when the electron is captured, the scissile C–O bond in the planar radical anion is strengthened by the increased C–O bonding contribution in the occupied molecular orbitals (spin density in the O atom). To achieve the cleavage, the $\sigma*$ spin molecular orbital of the C–O alkyl ether bond must be populated, and this would occur at the intersection region, provided that some coupling takes place between the two diabatic states. The scissile C–O bond stretching moves the molecule toward the intersection region, and the dihedral twisting away from planarity provides the coupling. The radical anion of the cyanophenyl benzyl ether (**2**) needs to lengthen the scissile C_8-O_7 bond from 1.441 Å up to 1.481 Å to reach that intersection region. Then, a Gibbs free energy barrier of 1.21 kcal/mol is required to reach the transition state.

Why is the intersection region energetically more difficult to reach in the case of **2** (homolytic mesolytic cleavage) than in the case of **1a** (heterolytic mesolytic cleavage)? The additional unpaired electron is mainly located in the cyanophenyl moiety of the molecule, and whatever migration of the electronic density toward the scissile C–O $\sigma*$ region requires potential energy, the farther away from the cyanophenyl ring the migration, the bigger the increment of potential energy. Considering the C atom provides the most important contribution to an antibonding $\sigma*$ molecular orbital, the migration of the unpaired electron to populate the C–O $\sigma*$ region (which is located essentially around the C atom) in the case of **2** happens to a somewhat farther away region than in the case of **1a**, where the C atom is directly attached to the cyanophenyl ring. In addition, our calculations (Figure 6) indicate that for **1a** the transition state can be reasonably represented as [•⁻NCArCH₂⁺⁻OPh]. Therefore, in this case, and according to Guthrie and Shi,[14b] the bond-polarized contributions to the transition state can make the intersection region easier to reach by allowing the extra electron to remain more localized in the π system than in the case of **2**.

4. General Discussion

Our electrochemical studies indicate that heterolytic mesolytic fragmentations of radical anions of 4-cyanobenzyl ethers have lower intrinsic barriers (more than 3 kcal/mol on average) than the related homolytic mesolytic fragmentations of radical anions of 4-cyanophenyl ethers. In the particular case of isomers 4-cyanobenzyl phenyl ether (**1a**) and 4-cyanophenyl benzyl ether (**2**), this difference ($\Delta\Delta G_0^{\#}$) amounts to 5.5 kcal/mol and produces an interesting energetic crossing since the thermodynamically more favorable process (cleavage of the radical anion

of product **2**, homolytic mesolytic cleavage, $\Delta\Delta G° = -6.2$ kcal/mol) is the kinetically slower one ($\Delta\Delta G^{\#} = 2.8$ kcal/mol). The fundamental reasons for this behavior have been established by means of theoretical calculations.

Even taking into account that the theoretical study has been performed in the gas phase, we have to underline that our theoretical calculations qualitatively agree and explain the experimental results in solution. Theoretically, both C–O alkyl ether cleavages turn out to be exergonic ($\Delta G° < 0$), with a clear thermodynamic advantage for the fragmentation of the radical anion of 4-cyanophenyl benzyl ether (**2**). Here also, the radical anion of 4-cyanobenzyl phenyl ether (**1a**) fragments faster than the radical anion of 4-cyanophenyl benzyl ether (**2**). The agreement between theory and experiment is qualitatively quite good when we compare the differences in Gibbs free energy barriers between **2** and **1a** ($\Delta\Delta G^{\#}$): 2.8 kcal/mol from experiment and 1.21 kcal/mol from theoretical calculation (assuming that the Gibbs free energy barrier for the fragmentation of the radical anion of **1a** is zero). Indeed, this indicates that any systematic error in the theoretical methodology has been canceled in the comparison of two very similar substrates (isomers). Certainly, the individual Gibbs free energy barriers in solution are significantly larger than what we obtain in the gas phase. However, the fact that $\Delta\Delta G^{\#}$ is very similar in the gas phase (theoretical calculations) and in solution (experiment) indicates that, in this particular case, the rate differences between the two fragmentation modes (and therefore the differences in intrinsic barriers) arise essentially from the fundamental features of the radical anion structures.

5. Conclusions

We have demonstrated that the clear thermodynamic advantage of the fragmentation of the radical anion of **2**, both in gas phase and in solution, is due to the fact that the factors that determine the kinetics of the aniomesolytic fragmentations are clearly different from those that control their thermodynamics. We have shown that kinetics depends on the features of the $\sigma*$ C–O alkyl ether region, which have no influence on the properties of the reactants or products. However, thermodynamics rather depends on the stabilizing effect of the electron-acceptor cyano substituent at the products, which indeed is clearly larger in the negatively charged cyanophenolate (one of the fragments coming from **2**) than in the neutral cyanobenzyl radical (one of the fragments resulting from **1a**). In other words, the introduction of the cyano substituent favors thermodynamically the fragmentation of the radical anion in which the oxygen atom is directly attached to the cyanophenyl ring (because this scission will lead to the cyanophenolate), but it favors kinetically the cleavage of the radical anion in which the carbon atom, which has the most important contribution to the $\sigma*$ C–O alkyl ether bond, is directly attached to the cyanophenyl ring.

Concerning the "spin regioconservation principle" (see Introduction), our results show that it can work as a mnemonic rule but that the real reasons for it to work are not related to the conservation of the spin density.

Our results suggest that the kinetic preference for heterolytic mesolytic fragmentation will be higher the more polarized the scissile bond is, and that the "spin regioconservation principle" will only hold for structures with highly polarized scissile bonds, where the kinetic advantage for the heterolytic mesolytic cleavage is able to overcome the thermodynamic tendency (homolytic mesolytic cleavage).

6. Experimental Section

Chemicals. All chemicals were purchased from Aldrich and were of the highest purity available. They were used as received. 4-Cyanobenzyl phenyl ether[37] (**1a**) and 4-cyanobenzyl methyl ether[38] (**1b**) were prepared and identified following previously described procedures.[39]

Instruments and Procedures. Cyclic voltammetry and electrolysis instruments and procedures have been previously described.[40] The electrochemical experiments were carried out at 20 °C. Digital simulations of the cyclic voltammetry curves were performed by using the DigiSim 2.0 software by Bioanalytical Systems Inc. The products from preparative electrolyses, toluonitrile, and phenol, were identified by comparison with commercial samples and the reactions were quantified by gas chromatography.

(37) (a) Penn, J. H.; Lin, Z. *J. Org. Chem*. **1990**, *55*, 1554. (b) Wagner, G.; Horn, H. *Pharmazie* **1975**, *30*, 353.
(38) (a) Tzeng, D.; Weber, W. P. *J. Org. Chem*. **1981**, *46*, 265. (b) Eliel, E. L.; Badding, V. G.; Rerick, M. N. *J. Am. Chem. Soc*. **1962**, *84*, 2371.
(39) Kornblum, N.; Lurie, A. P. *J. Am. Chem. Soc*. **1959**, *81*, 2705.
(40) (a) Andrieux, C. P.; Larumbe, D.; Gallardo, I. *J. Electroanal. Chem*. **1991**, *304*, 241. (b) Andrieux, C. P.; Batlle, A.; Espín, M.; Gallardo, I.; Jiang, Z.; Marquet, J. *Tetrahedron*, **1994**, *50*, 6913. (c) Gallardo, I.; Guirado, G., Marquet, J. *J. Electroanal. Chem*. **2000**, *488*, 64. (d) Gallardo, I.; Guirado, G.; Marquet, J. *Chem. Eur. J.* **2001**, *7*, 1759.